SIRT2-Mediated ACSS2 K271 Deacetylation Suppresses Lipogenesis Under Nutrient Stress

Rezwana Karim[1], Wendi Teng[1], Cameron Behram[1], Hening Lin[1,2]
[1]Department of Chemistry and Chemical Biology, Cornell University, Ithaca, New York, USA.
[2]Howard Hughes Medical Institute; Department of Chemistry and Chemical Biology; Department of Molecular Biology and Genetics, Cornell University, Ithaca, New York, USA.
Correspondence: hl379@cornell.edu.

Abstract

De novo lipogenesis is associated with the development of human diseases such as cancer, diabetes, and obesity. At the core of lipogenesis lies acetyl coenzyme A (CoA), a metabolite that plays a crucial role in fatty acid synthesis. One of the pathways contributing to the production of cytosolic acetyl-CoA is mediated by acetyl-CoA synthetase 2 (ACSS2). Here, we reveal that when cells encounter nutrient stress, particularly a deficiency in amino acids, Sirtuin 2 (SIRT2) catalyzes the deacetylation of ACSS2 at the lysine residue K271. This results in K271 ubiquitination and subsequently proteasomal degradation of ACSS2. Substitution of K271 leads to decreased ubiquitination of ACSS2, increased ACSS2 protein level, and thus increased lipogenesis. Our study uncovers a mechanism that cells employ to efficiently manage lipogenesis during periods of nutrient stress.

Introduction

Cellular metabolism is influenced by various factors, including diet, stress, and genetics, which can have significant implications for health[1]. Dysregulation of these factors has been linked to the development of diseases such as cancer, diabetes, and obesity[2,3]. Among the metabolic pathways affected by these disturbances, de novo lipogenesis (DNL) stands out. DNL underlies the pathogenesis of non-alcoholic fatty liver disease and obesity, and is also exacerbated in cancer[1,4]. Therefore, gaining a comprehensive understanding of DNL and its regulatory mechanisms is of utmost importance.

At the core of DNL lies acetyl coenzyme A (acetyl-CoA), a fundamental metabolite that serves as a building block for fatty acid biosynthesis[5]. Two primary pathways contribute to the production of cytosolic acetyl-CoA. One pathway is governed by the enzyme ATP citrate lyase (ACLY), which converts citrate derived from the mitochondrial tricarboxylic acid (TCA) cycle into acetyl-CoA for DNL[6,7]. The second pathway involves acetyl-CoA synthetase 2 (ACSS2), which catalyzes the ligation of exogenous acetate to CoA, generating acetyl-CoA in an ATP-dependent reaction[8,9]. While acetate is not typically a fuel source in mammalian cells, its uptake increases under conditions of stress, such as low oxygen and nutrient availability[5,10]. In the metabolically stressed tumor microenvironment, ACSS2 promotes malignant cell growth by allowing cells to utilize acetate as an additional nutritional source when other carbon sources are scarce[9,11,12]. Consequently, ACSS2 has been found to be upregulated in various cancers, including breast and hepatic cancer[8,11,13]. Recent studies have implicated ACSS2 in promoting

the progression of hepatic steatosis, a condition defined by aberrant fat build up in the liver[14]. In a diet induced obesity model, mice lacking ACSS2 exhibited a significant reduction in body weight, serum cholesterol as well as lower hepatic triglyceride levels[14]. These findings underscore the significance of ACSS2 in metabolism and motivate us to further explore the mechanisms regulating its function.

Lysine acetylation is gaining recognition as a key regulator of metabolic processes by modifying and impacting metabolic enzymes. Most cytosolic and nuclear lysine acetylation is installed by a set of acetyltransferases, including p300/CBP, PCAF, and HAT1, while the enzymes for most mitochondrial lysine acetylation events remain unknown[15]. Lysine acetylation is reversible and can be removed by members of the metal ion-dependent histone deacetylases (HDAC1-11) or NAD^+- dependent sirtuin (SIRT1-SIRT7) family of enzymes[16]. The catalytic activity of ACSS2 was reported to be inhibited by lysine acetylation on K661 and activated by SIRT1-catalyzed deacetylation[17,18]. In our present study, we elucidate a new regulation of ACSS2 by lysine acetylation. Specifically, SIRT2 deacetylates ACSS2 at a specific lysine residue, K271, in response to nutrient stress. This deacetylation event exposes K271 for subsequent ubiquitination, ultimately marking ACSS2 for degradation. This degradation process results in a reduction in fatty acid synthesis, thereby revealing a previously unknown mechanism through which mammalian cells down regulate DNL via ACSS2 deacetylation, ubiquitination, and proteasomal degradation under conditions of nutrient stress.

Results

SIRT2 Deacetylates ACSS2 under nutrient and amino acid deficiency. Hallows et al. revealed that ACSS2 undergoes deacetylation mediated by SIRT1, a class III deacetylase[17]. Among the seven known class III deacetylases in mammalian cells (Sirt1-7), SIRT1 and SIRT2 are the major cytosolic members[19–21]. Given the cytosolic localization of ACSS2, we were interested in investigating whether SIRT2 could also serve as a potential deacetylase for ACSS2. To address this, we ectopically expressed Flag-tagged ACSS2 and HA-tagged SIRT2 in HEK293T cells[22]. We performed immunoprecipitation experiments using anti-acetyl-lysine beads to capture lysine-acetylated proteins, and the acetylation level of ACSS2 was assessed using an anti-Flag antibody. Our results demonstrated that the expression of SIRT2 led to a decrease in ACSS2 acetylation, indicating that SIRT2 is capable of deacetylating ACSS2 (Figure 1A).

To investigate whether endogenous SIRT2 regulates the acetylation levels of ACSS2, we employed lentiviral-mediated expression of short hairpin RNA (shRNA) to knock down SIRT2 in HEK293T cells. We then immunoprecipitated ectopically expressed Flag-tagged ACSS2 from both control and SIRT2 knockdown cells. However, we did not observe any significant difference in ACSS2 acetylation levels upon SIRT2 knockdown (Figure 1B). We hypothesized that this could be due to the low basal levels of SIRT2 in cells, which might not yield a substantial deacetylation effect detectable by western blotting. SIRT2 has been reported to be upregulated under various stress conditions, including Golgi stress induced by shigella infection[23,24] as well as under conditions of low glucose or amino acid deprivation[24,25]. To induce

a stress response that would upregulate SIRT2 and potentially affect ACSS2 acetylation, we subjected cells to nutrient exhaustion by not changing the cell culture media over the course of four days [26].This resulted in an increase in SIRT2 levels (Figure S1) and when SIRT2 was knocked down under this condition, ACSS2 had increased acetylation compared to control knockdown cells (Figure 1B). These findings suggest that the deacetylation of ACSS2 by SIRT2 happens in the context of nutrient stress.

Our initial approach of inducing nutrient exhaustion could be due to a multitude of factors hence we wanted to deconvolute the specific nutrient stress that led to the enhanced deacetylation of ACSS2. Because previous reports showed that SIRT2 is upregulated under conditions of low glucose or amino acid deprivation[24,27], we examined the changes in ACSS2 acetylation in SIRT2 control and knockdown cells under these conditions. We observed that under amino acid deprivation, SIRT2 knockdown increased ACSS2 acetylation levels (Figure 1C). Notably, this effect was not observed under glucose starvation, underscoring the specificity of SIRT2's deacetylation activity to amino acid stress (Figure S2). To further confirm the effect of SIRT2 on ACSS2 acetylation, we employed the SIRT2-specific small molecule inhibitor thiomyristoyllysine (TM) (Figure S3). ACSS2 acetylation increased under amino acid-starved conditions but not under normal conditions. These findings align with a previous study demonstrating that amino acid starvation triggers SIRT2 activation and subsequent deacetylation of ATG4B[27]. Overall, our data indicates that SIRT2 deacetylates ACSS2 in response to nutrient stress, particularly amino acid deprivation.

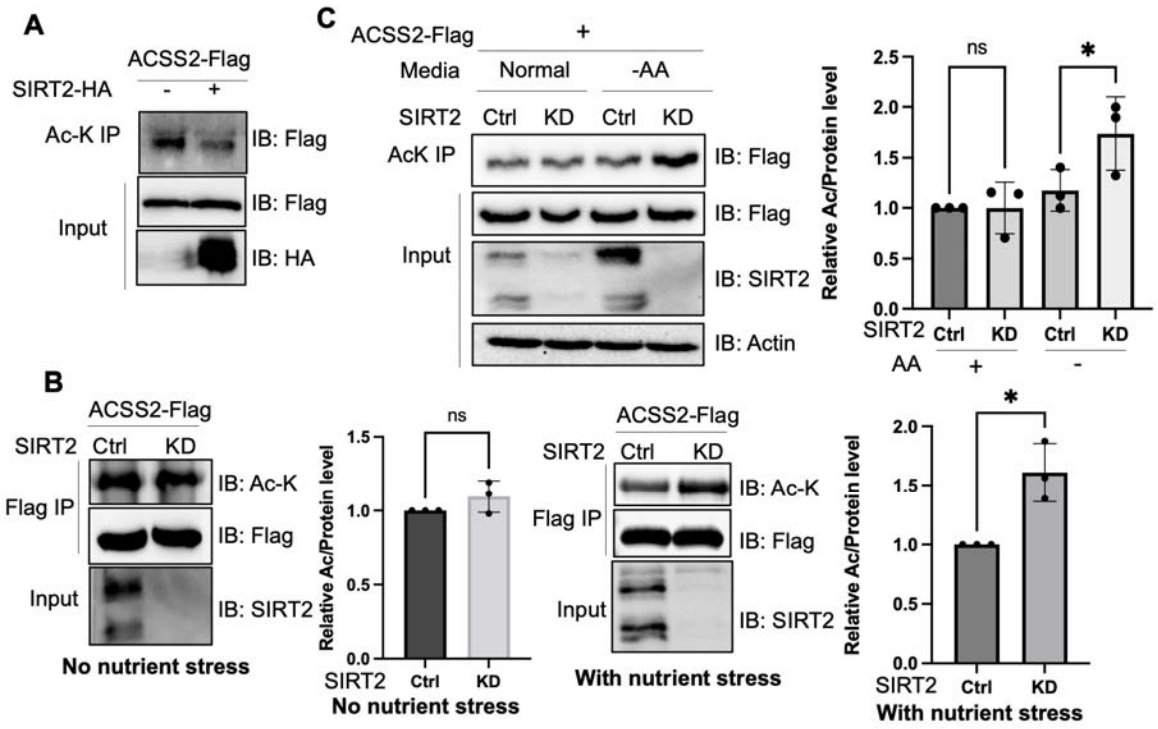

Figure 1. Deacetylation of ACSS2 by SIRT2 under nutrient and amino acid stress. (**A**) Overexpression of SIRT2 decreases ACSS2 acetylation. Flag-tagged ACSS2 was co-transfected with HA-tagged SIRT2 into HEK 293T cells. Acetylation was determined using acetyl lysine IP and then western blot for Flag-ACSS2. (**B**) ACSS2 is deacetylated

by SIRT2 under nutrient stress. Flag-tagged ACSS2 was ectopically expressed in control and SIRT2 knockdown HEK 293T cells. SIRT2 knockdown only increased ACSS2 acetylation under nutrient stress. Relative acetylation/Flag ratios were quantified. Error bars represent ±SD for experiments performed in triplicate ** indicating $p<0.01$. (**C**) ACSS2 is deacetylated by SIRT2 under amino acid deprivation. Flag-tagged ACSS2 was ectopically expressed in control and SIRT2 knockdown HEK 293T cells. One set was grown in normal media and one set in EBSS media (no amino acids). Changes in ACSS2 acetylation was determined by acetyl lysine IP and western blot for Flag. Relative acetylation/Flag ratios were quantified. Error bars represent ±SD for experiments performed in triplicate ** indicating $p<0.01$.

Acetylation stabilizes ACSS2 by inhibiting ubiquitination. We next aimed to investigate how nutrient stress induced ACSS2 deacetylation by SIRT2 affects ACSS2 function. Consistent with the acetylation data, we found no alterations in the endogenous levels of ACSS2 when SIRT2 was knocked down under normal conditions. However, in the presence of nutrient stress, the endogenous ACSS2 levels exhibited an increase upon SIRT2 knockdown (Figure 2A). This effect was replicated under amino acid starvation (Figure 2B, S4) conditions but not under glucose starvation (Figure S2). This was replicated in A549 cells as well (Figure S5). To further investigate this phenomenon, we used cycloheximide to inhibit translation and assess the stability of ACSS2 under amino acid limitation. We found that ACSS2 exhibited lower stability in the presence of amino acid limitation compared to normal culturing conditions (Figure S6). This suggests that under amino acid limitation, when SIRT2 is more active, there is an increased rate of deacetylation and degradation of ACSS2. Furthermore, our data demonstrated that under amino acid limitation, knocking down SIRT2 led to the stabilization of ACSS2 (Figure 2C, S7). Importantly, ACSS2 mRNA levels remained largely unaffected by SIRT2 knockdown or amino acid starvation, indicating that the upregulation of ACSS2 by SIRT2 knockdown primarily occurs at the post-transcriptional level (Figure S8). This suggests that SIRT2-mediated deacetylation of ACSS2 under amino acid limitation promotes its degradation, revealing a potential mechanism by which nutrient stress modulates ACSS2 function.

To elucidate the mechanism via which acetylation regulates ACSS2 protein levels, we initially examined whether it undergoes degradation via the lysosome or the proteasome. We treated cells with bafilomycin (Baf), which inhibits lysosomal acidification, and MG132, a proteasome inhibitor[28,29]. Endogenous ACSS2 levels increased with MG132 treatment but not with Baf, indicating that ACSS2 is degraded through the proteasomal pathway (Figure 2D, S9). Moreover, we readily observed ubiquitination of Flag-ACSS2 (Figure 2E). Given that SIRT2 knockdown increased endogenous ACSS2 levels, we further investigated whether SIRT2 regulates the ubiquitination of ACSS2. Notably, we found that knockdown or inhibition of SIRT2 in amino acid deprived media led to a decrease in ACSS2 K48-linked ubiquitination (Figure 2F and 2G), a hallmark of proteasomal degradation, suggesting that SIRT2 regulates the ubiquitination and degradation of ACSS2 through the proteasome pathway[30]. The data together suggest that SIRT2 deacetylates ACSS2 to promote its ubiquitination and proteasomal degradation.

To further confirm this model and investigate the physiological significance of ACSS2 regulation by SIRT2, we aimed to identify the specific lysine residue deacetylated by SIRT2. Utilizing label-free quantification mass spectrometry, we analyzed purified Flag-tagged ACSS2 from control and SIRT2 knockdown cells. Our analysis showed that ACSS2 acetylation levels at

K271 increased in SIRT2 knockdown cells (Table S1). SIRT2 knockdown failed to affect the acetylation level for the K271R mutant in amino acid deprived media, indicating that K271 is the site of deacetylation by SIRT2 (Figure 2H). In contrast, the acetylation level of ACSS2 K661R mutant was still regulated by SIRT2 (Figure S10). These observations collectively indicate that SIRT2 deacetylates ACSS2 at K271, which is different from previously reported SIRT1-regulated K661 deacetylation.

Interestingly, data from the global characterization of the ubiquitin-modified proteome indicated that ACSS2 can be ubiquitinated at the K271[31]. To validate this, we tested the K48-linked ubiquitination of K271R and K271Q mutants, and both mutants showed a decrease in ACSS2 ubiquitination levels (Figure S11). SIRT2 knockdown in amino acid deprived media decreased the ubiquitination of WT ACSS2, but not the ubiquitination of the K271R mutant (Figure 2I). Furthermore, the K271R mutant exhibited enhanced stability compared to the wild-type ACSS2 when cells were cultured in EBSS medium lacking amino acids (Figure 2J). Collectively, our findings suggest that under amino acid limitation, SIRT2 deacetylates K271, thereby exposing the site for ubiquitination and leading to subsequent degradation of ACSS2.

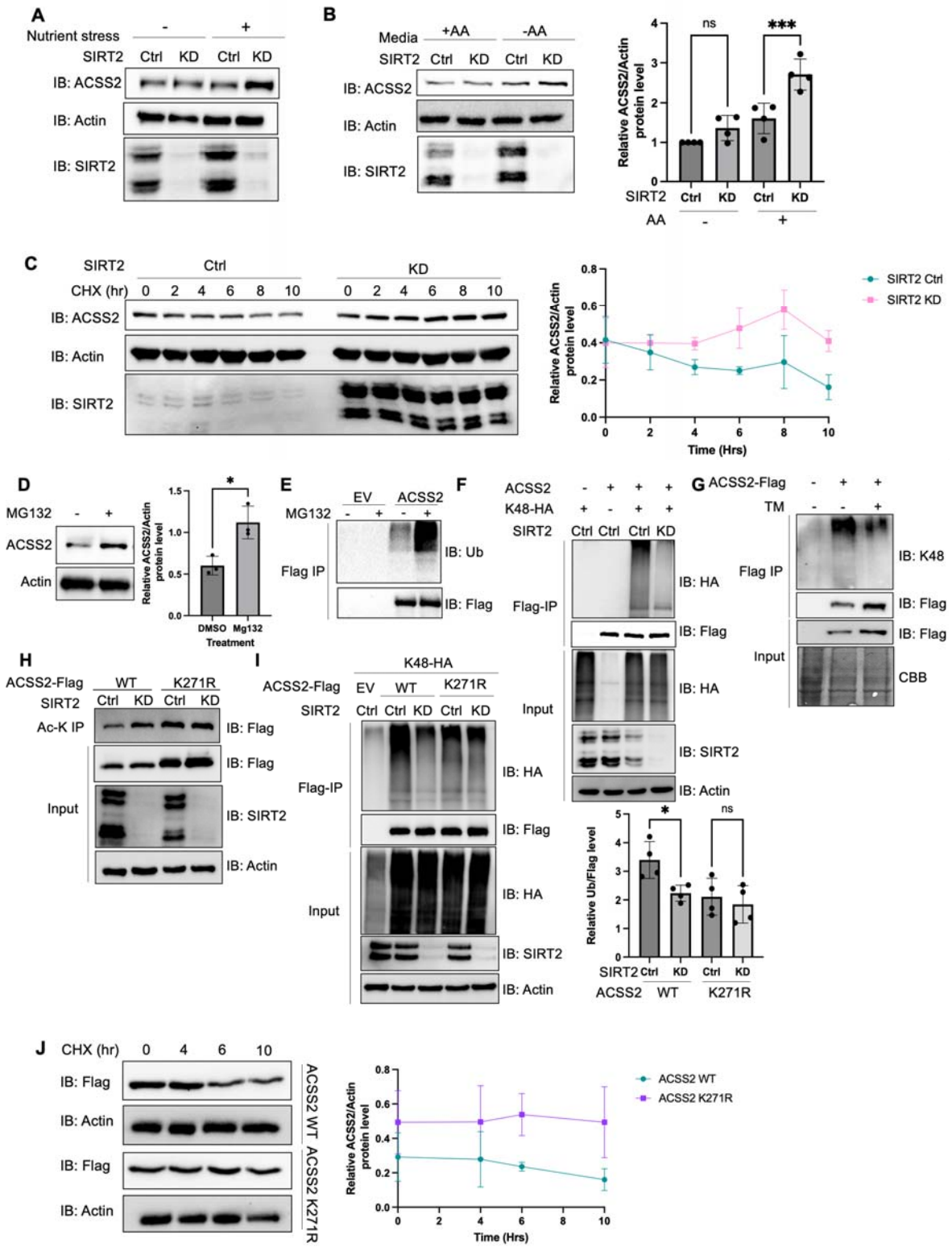
A
Nutrient stress
-
+
SIRT2
Ctrl
KD
Ctrl
KD
IB: ACSS2
IB: Actin
IB: SIRT2
B
Media
+AA
-AA
SIRT2
Ctrl
KD
Ctrl
KD
IB: ACSS2
IB: Actin
IB: SIRT2
ns
***
Relative ACSS2/Actin protein level
SIRT2
Ctrl
KD
Ctrl
KD
AA
-
+
C
SIRT2
Ctrl
KD
CHX (hr)
0 2 4 6 8 10
0 2 4 6 8 10
IB: ACSS2
IB: Actin
IB: SIRT2
Relative ACSS2/Actin protein level
Time (Hrs)
SIRT2 Ctrl
SIRT2 KD
D
MG132
-
+
ACSS2
Actin
Relative ACSS2/Actin protein level
*
DMSO
Mg132
Treatment
E
EV
ACSS2
MG132
-
+
-
+
Flag IP
IB: Ub
IB: Flag
F
ACSS2
-
+
+
+
K48-HA
+
-
+
+
SIRT2
Ctrl
Ctrl
Ctrl
KD
Flag-IP
IB: HA
IB: Flag
Input
IB: HA
IB: SIRT2
IB: Actin
G
ACSS2-Flag
-
+
+
TM
-
-
+
Flag IP
IB: K48
IB: Flag
Input
IB: Flag
CBB
H
ACSS2-Flag
WT
K271R
SIRT2
Ctrl
KD
Ctrl
KD
Ac-K IP
IB: Flag
IB: Flag
Input
IB: SIRT2
IB: Actin
I
K48-HA
ACSS2-Flag
EV
WT
K271R
SIRT2
Ctrl
Ctrl
KD
Ctrl
KD
Flag-IP
IB: HA
IB: Flag
Input
IB: HA
IB: SIRT2
IB: Actin
*
ns
Relative Ub/Flag level
SIRT2
Ctrl
KD
Ctrl
KD
ACSS2
WT
K271R
J
CHX (hr)
0
4
6
10
IB: Flag
IB: Actin
IB: Flag
IB: Actin
ACSS2 WT
ACSS2 K271R
Relative ACSS2/Actin protein level
Time (Hrs)
ACSS2 WT
ACSS2 K271R

Figure 2. K271 acetylation shields ACSS2 from proteasomal degradation by impeding K271 ubiquitination. (**A** and **B**) Endogenous ACSS2 levels increase when SIRT2 was knocked down under nutrient and amino acid stress. SIRT2 control and knock down HEK 293T cells were maintained in normal and nutrient deprived (**A**) or EBSS (**B**) media and endogenous ACSS2 protein levels were determined by western blot. Relative ACSS2/Actin ratios were quantified. ACSS2 level quantification was relative to Actin. Error bars represent ±SD for experiments performed in triplicate. (**C**) Knockdown of SIRT2 stabilizes ACSS2 in amino acid deprived media. SIRT2 control and knockdown HEK293T cells were maintained under EBSS media and treated with CHX at the indicated time points. Endogenous ACSS2 level was determined by western blot and quantified. Error bars represent SD for experiments performed in triplicate. (**D**) Endogenous ACSS2 accumulated by treatment of proteasome inhibitor MG132. HEK293T cells were treated with or without MG132. Cells were treated with EBSS media. Endogenous ACSS2 level was determined by western blot and quantified. Error bars represent SD for experiments performed in triplicate. (**E**) ACSS2 is ubiquitinated. Flag-tagged ACSS2 was transfected into HEK 293T cells. The cells were then treated with MG132. Ubiquitination of immunoprecipitated ACSS2 was determined using a pan-ubiquitin antibody. (**F**) Knockdown of SIRT2 decreases ACSS2 ubiquitination. Flag-ACSS2 was co-transfected with HA-tagged K48 ubiquitin into SIRT2 control and knockdown HEK 293T cells. Cells were maintained in EBSS media. Ubiquitination of purified Flag-ACSS2 was analyzed by western blot. (**G**) Inhibition of SIRT2 with TM decreases ACSS2 ubiquitination. Flag-tagged ACSS2 was transfected into HEK 293T cells with or without TM treatment. Cells were maintained in EBSS media. Ubiquitination of immunoprecipitated protein was detected using K48 ubiquitin antibody. (**H**) SIRT2 deacetylates ACSS2 at K271. Flag-tagged ACSS2 wildtype and K271R mutant were ectopically expressed in control and SIRT2 knockdown HEK 293T cells. Cells were maintained in EBSS media. Acetylation levels was detected by western blot. (**I**) Knockdown of SIRT2 does not change K271R ACSS2 ubiquitination. Flag-tagged WT and K271R ACSS2 were co-transfected with HA-tagged K48 ubiquitin into SIRT2 control and knockdown HEK 293T cells. Ubiquitination of purified proteins was analyzed by western blot and quantified. Ubiquitination quantification is relative to Flag-tag. Error bars represent SD for experiments performed in triplicate. (**J**) ACSS2 K271R mutant is more stable than WT. Flag-tagged ACSS2 WT or K271R mutant were ectopically expressed in HEK 293T cells. Cells were treated with CHX to inhibit protein synthesis. The levels of the WT and K271R mutant ACSS2 at different time points were determined by western blot and quantified. Error bars represent SD for experiments performed in triplicate.

Acetylation of ACSS2 promotes De Novo Lipogenesis. ACSS2 is known to be involved in de novo lipogenesis. Deletion of ACSS2 in mice results in reduced body weight and lipid deposition, while mutation of S236, a phosphorylation site on ACSS2, leads to increased triglyceride levels in adipocytes[14,32]. Based on our finding that ACSS2 is deacetylated and regulated by SIRT2, we next wanted to test whether this regulation could play a role in de novo lipogenesis.

To investigate this, we conducted a knockdown of endogenous ACSS2 in 3T3-L1 preadipocytes and reintroduced either wild-type or the K271R mutant ACSS2 through transfection. To ensure comparable expression levels at the beginning, we adjusted the amount of transfected DNA for both wild-type and the K271R mutant ACSS2. Western blot analysis confirmed the successful knockdown of ACSS2 and the restoration of ACSS2 expression levels with both the wild-type and K271R mutant (Figure 3A). The cells were then subjected to adipocyte differentiation protocol. After 7 days, we observed that the protein level of the K271R mutant was higher than that of the wild type ACSS2 (Figure 3B). This is consistent with our finding above that K271R mutation suppresses the ubiquitination and degradation of ACSS2.

We determined the lipogenesis with Oil Red O staining, which detects lipid droplets in cells. During the differentiation process, we supplemented the media with acetate to induce lipogenesis through the ACSS2 pathway. Additionally, post differentiation and before reading

out the Oil Red O staining, we cultured the cells for three more days without changing media to have a nutrient limiting condition. In the ACCS2 knockdown cells, re-expression of WT ACSS2 increased lipid accumulation based on Oil Red O staining of differentiated adipocytes, thereby validating ACSS2's functional role in de novo lipogenesis. Consistent with our above observation that ACSS2 K271R mutant is more stable than the WT, expressing the K271R mutant lead to more lipid droplets than expressing the WT ACSS2 (Figure S12).

To find out whether SIRT2-mediated deacetylation of ACSS2 K271 affect lipogenesis, we used the SIRT2 small molecule inhibitor, TM. The inhibition of SIRT2 using TM increased lipid accumulation in cells with WT ACSS2, but not in cells with the K271R mutant that cannot be deacetylated by SIRT2 (Figure 3C and D). To make sure the mutants were enzymatically active, we isolated Flag-tagged wildtype, K271R, and K271Q ACSS2 proteins from SIRT2 knockdown HEK293T cells. Subsequently, we examined acetyl-CoA formation from acetate and CoA using high-performance liquid chromatography (HPLC). Our findings indicate that while the wildtype ACSS2 exhibits slightly higher activity compared to the K271R and K271Q mutants, all variants remain functional (Figure S13). The slight reduction in acetyl-CoA formation for the K271R mutant may explain the relatively modest increase in lipid droplet formation observed in Figure 3D. These findings are consistent with the model that SIRT2 deacetylates ACSS2 on K271 to promote ACSS2 ubiquitination and degradation, and thus inhibiting lipogenesis (Figure 4).

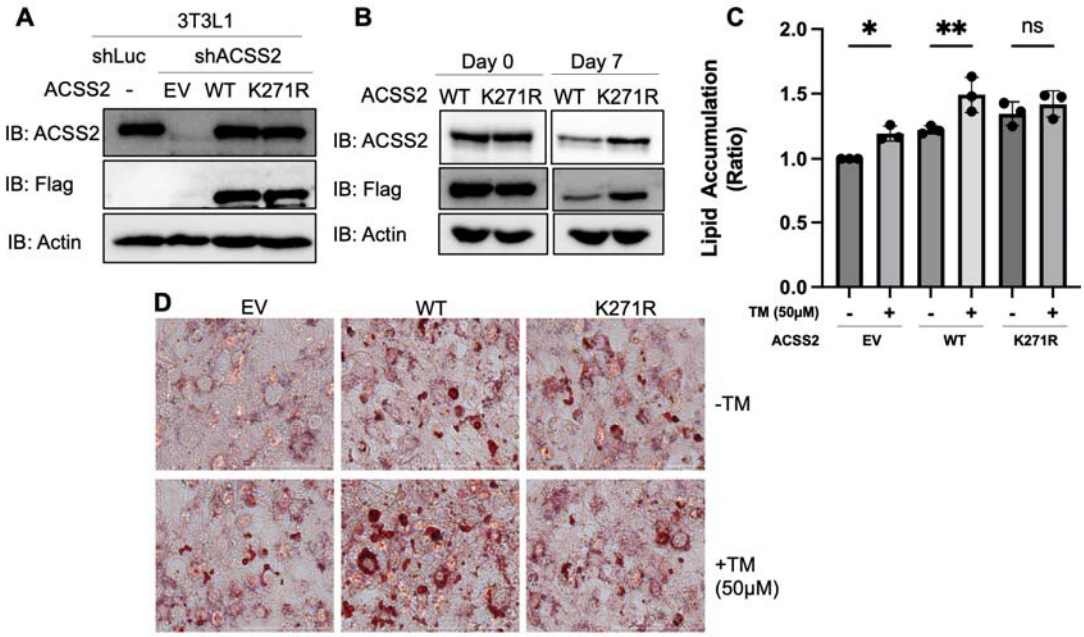

Figure 3. Acetylation of ACSS2 at K271 promotes lipid accumulation. (**A**) Endogenous ACSS2 was stably knocked down with shRNA in 3T3L1 cells and then wildtype or K271R mutant of ACSS2 was re-expressed in the knockdown cells to a level that is compatible with endogenous ACSS2. ACSS2 knockdown efficiency and re-expression levels were determined by western blot. (**B**) The cell lysate at day 0 and 7 were collected and ACSS2 level was measured by western blot. (**C, D**) Inhibition of SIRT2 with TM results in increased neutral lipid accumulation in cells expressing ACSS2 WT but not in cells expressing ACSS2 K271R mutant. The differentiation media was supplemented with 1.5 mM acetate. Accumulation of neutral lipids in differentiated adipocytes was measured using Oil Red O. Neutral lipid accumulation is quantified (C) by measuring the absorbance of stained neutral lipids at 500

nm on a plate reader. Representative cell imaging is shown in (D). Statistical analysis was performed using an unpaired two-tailed Student's t-test, with * indicating $p<0.05$ and ** indicating $p<0.01$.

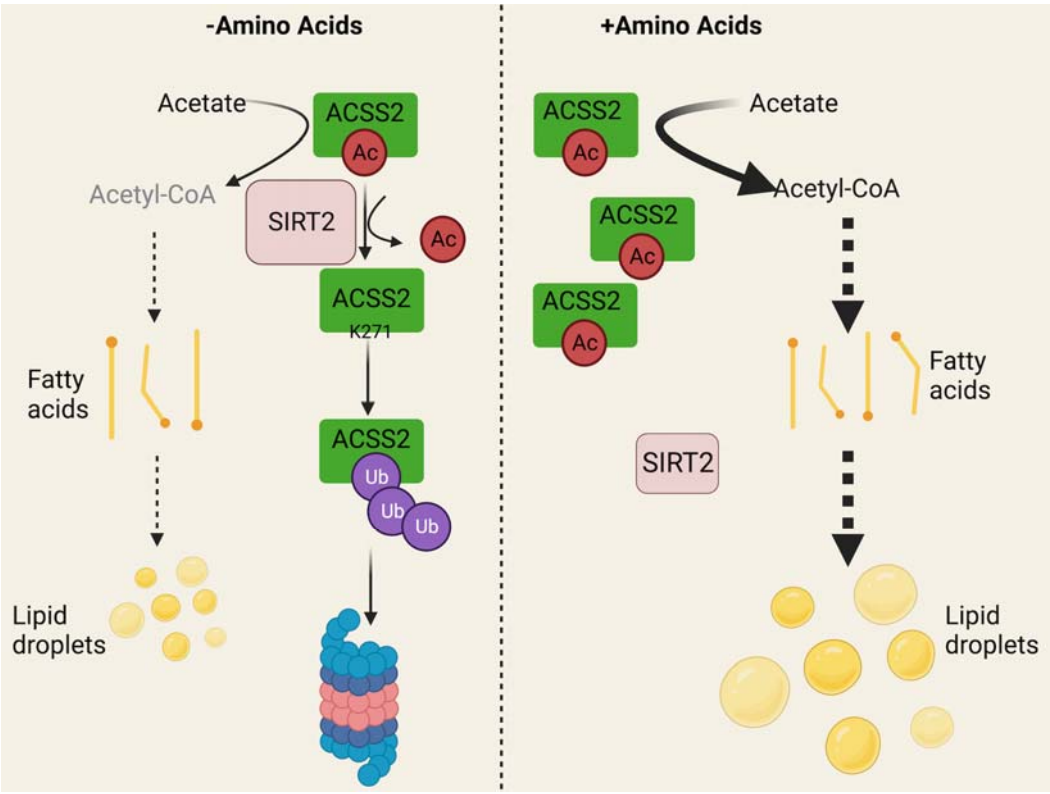

Figure 4. Working model. Under amino acid stress, SIRT2 actively deacetylates ACSS2 at K271, which reveals the site for ubiquitination and leads to the degradation of ACSS2. This downregulation of ACSS2 protein level results in decreased de novo lipogenesis (DNL). On the contrary, without amino acid stress, acetylation at K271 protects ACSS2 from degradation resulting in higher DNL. Created with BioRender.com

Discussion

Our study here identified ACSS2 K271 as a new substrate for SIRT2-mediated deacetylation. Interestingly, SIRT2-mediated ACSS2 K271 deacetylation only becomes obvious/important during nutrient (amino acid) limitation. K271 deacetylation leads to the ubiquitination and degradation of ACSS2, resulting in reduced lipogenesis (see working model in Figure 4). This regulatory mechanism can help to maintain cellular homeostasis by limiting lipogenesis under amino acid limitation. SIRT2 has been reported to be upregulated by several stresses, including Golgi stress caused by bacterial infection and nutrient depletion.[23,24] Thus, SIRT2 is increasingly recognized as a stress response protein. Our study here provides an interesting mechanism through which cells senses one metabolic stress (amino acid limitation) to regulate a different metabolic pathway (lipogenesis) by calling on SIRT2.

De novo lipogenesis is a tightly regulated metabolic pathway responsible for converting excess carbons derived from carbohydrates or amino acids into fatty acids, contributing to triglyceride synthesis and storage. Dysregulation of DNL is associated with metabolic disorders such as obesity and non-alcoholic fatty liver disease. SIRT2 has been implicated in the regulation of DNL[33]. SIRT2 is widely expressed in metabolically active tissues including adipose tissue and exerts its influence on DNL through the deacetylation of several proteins[34]. One important target of SIRT2 deacetylation is FoxO1, a transcription factor involved in adipogenesis. During calorie restriction, SIRT2-mediated deacetylation of FoxO1 promotes its nuclear localization, where it suppresses the transcription of PPARγ, a master regulator of adipocyte differentiation[25,35,36]. SIRT2 also suppresses ACLY, an enzyme responsible for the conversion of citrate to acetyl-CoA for fatty acid synthesis. SIRT2-mediated degradation of ACLY decreases acetyl-CoA production, thereby inhibiting DNL[37,38]. Our finding here revealed that SIRT2 could also regulate another protein involved in DNL, ACSS2. Thus, it seems that SIRT2 can inhibit DNL through deacetylating many different substrate proteins.

ACSS2 has been reported to be activated by SIRT1-catalyzed deacetylation on K661.[17] Subsequently, a follow-up investigation unveiled the role of the circadian clock in modulating intracellular acetyl-CoA levels through regulation of ACSS2 enzymatic activity. This study demonstrated the cyclic nature of ACSS2 acetylation, with rhythmicity dependent on a functional circadian clock. Specifically, deacetylation of K661 by SIRT1 was found to activate ACSS2, leading to periodic increases in acetyl-CoA production[18]. Conversely, our research elucidates a contrasting mechanism wherein SIRT2 inhibits ACSS2 by deacetylating K271 under conditions of nutrient stress. The dual regulation of ACSS2 by SIRT1 through the circadian clock and SIRT2 under nutrient stress underscores the intricate and multifaceted nature of regulatory mechanisms involved in lipid metabolism. These findings underscore the versatility of lysine acetylation in modulating cellular metabolic pathways.

Furthermore, our study is complemented by research demonstrating the interconnection of metabolic pathways in response to nutrient levels. For instance, Guo et al. found that GCN2 kinase, which responds to amino acid scarcity, regulates lipid metabolism by suppressing lipogenesis in response to amino acid deprivation[41]. This highlights the intricate interplay between amino acid metabolism and lipid metabolism, further emphasizing the significance of understanding the regulatory mechanisms involving enzymes like ACSS2 in various metabolic contexts. Collectively, these studies contribute to a better understanding of how SIRT1 and SIRT2 regulate ACSS2 activity in various metabolic contexts, thereby enhancing our knowledge of acetate metabolism and its implications in health and disease.

Our study provides further support for the important roles of SIRT2 in curbing DNL. DNL underlies many human diseases, including obesity and non-alcoholic liver disease[42]. Given the role of SIRT2 in suppressing DNL, methods that can increase SIRT2 activity or protein levels may be useful for treating human diseases involving DNL.

Methods

Reagents. Anti-FLAG affinity gel (A2220), anti-FLAG antibody conjugated with horse radish peroxidase (A8592,1:10000) and HA antibody (SAB4300603,1:1000) were purchased from Sigma-Aldrich. Antibody against β-actin (sc-4777, 1:1000) was purchased from Santa Cruz Biotechnology. Anibodies against SIRT2 (D4050,1:1000), ACSS2 (D19C6, 1:1000), Ubiquitin (E4I2J, 1:1000), K48-linkage Specific Polyubiquitin (#4289, 1:1000) were purchased from Cell Signaling Technology. PTM antibodies anti-Kac (cat. #PTM-101) were purchased from PTM Biolabs Inc. (Chicago, IL). Protease inhibitor cocktail, bafilomycin A1, cycloheximide and adipocyte differentiation cocktail was purchased from Sigma-Aldrich. ECL plus western blotting detection was purchased from Thermo Scientific. Polyethyleneimine (PEI) was purchased from Polysciences (24765). MG132 was purchased from Cayman. TM was made as previously described[43].

Cloning and Mutagenesis. ACSS2 expression vector with FLAG tag (NM_018677) was purchased from Origene (Rockville, MD) for mammalian expression. To create ACSS2 K271 mutant constructs, site-directed mutagenesis via Quick Change PCR amplification was performed using the following primers: K271R Forward: 5'-CAGTCCCCCCCAATTAGG AGGTCATGCCCAGAT-3' Reverse: 5'- CCTAATTGGGGGGGACTGGCTGGTGGAGTCACC-3'. K271Q Forward: 5' -CAGTCCCCCCCAATT CAG AGGTCATGCCCAGAT-3'. Reverse: 5'-CTGAATTGGGGGGGACTGGCTGGTGGAGTCACC-3'

pRK5-HA-Ubiquitin-K48 was a gift from Ted Dawson (Addgene plasmid # 17605; http://n2t.net/addgene:17605 ; RRID:Addgene_17605).

SIRT2 wildtype and H187Y mutant expression vector with FLAG tag was made as previously described[44].

Immunoblotting. ACSS2 expression plasmid was transfected into HEK293T cells using PEI transfection reagent following the manufacturer's protocol. The pCMV-Tag4a empty vector was used as the negative control. After overnight transfection, cells were washed twice with ice cold PBS and collected by centrifugation at 1000 g for 5 min. Cells were then lysed in 1 mL of 1% NP-40 lysis buffer (25 mM Tris−HCl, pH 7.8, 150 mM NaCl, 10% glycerol and 1% NP-40) with protease inhibitor cocktail (1:100 dilution) by rocking at 4°C for 30 min. After centrifugation at 17,000 g for 30 min, the supernatant was collected, and protein concentration was determined with the Bradford assay (23200, Thermo Fisher). Normalized Lysates were incubated with 20μL of anti-FLAG affinity gel or anti-Acetyl-Lysine (mAb mix) Affinity Beads (Cytoskeleton, Inc., AAC04-beads) at 4°C for 2 h. The affinity gel was washed three times with washing buffer (25 mM Tris−HCl, pH 7.8, 150 mM NaCl, 0.2% NP-40). Beads were dried with gel loading tips and resuspended in 30μL of 1x SDS loading dye. Western blot analysis was carried out according to standard methods.

Cell Culture. HEK293Tcells were cultured in DMEM media (11965−092, Gibco) with 10% calf serum (C8056, Sigma-Aldrich). SIRT2 stable knockdown HEK293T cells were generated as previously described. Cells were washed with phosphate buffer saline (PBS) 24 hours post transfection and grown in Earle's Balanced Salt Solution (EBSS) (24010043, Thermo Fisher) with 10% calf serum for 16 hours to induce amino acid stress.

3T3-L1 (American Type Culture Collection, ATCC, Manassas, VA) preadipocytes were cultured in high-glucose (400 mg/dl) Dulbecco's modified Eagle's medium (DMEM, 11965–092, Gibco) containing 10% fetal bovine serum (FBS, 26140079, Gibco). For ACSS2 shRNA stable knockdown, lentivirus was generated by cotransfection of pLKO.1 with shRNA sequences specific to ACSS2 (TRCN0000045563, Millipore), pCMV-dR8.2,and pMD2.G plasmids into HEK293T cells. The cell medium was collected 48 h after transfection and used to infect early passage cultures of 3T3L1 cells. After 72 h, infected cells were treated with1.5μg/mL puromycin to select for stably incorporated shRNA constructs. The empty pLKO.1 vector was used as a negative control. ACSS2 wildtype and K271R mutant Flag-tagged expression plasmids were transfected into ACSS2 knockdown 3T3-L1 cells using PEI transfection reagent following the manufacturer's protocol. The pCMV-Tag4a empty vector was used as the negative control. Differentiation of 3T3L1 cell lines were done according to manufacturer's protocol (DIF001-1KT, Sigma Aldrich) 24 hours after transfection. Differentiation media was supplemented with 1.5 mM acetate (S5636, Sigma Aldrich) and the cells were cultured for three days more post differentiation without changing media to mimic a nutrient limiting condition. Oil Red O (ORO) of the differentiated cells was carried out according to standard protocol.

Detection of acetylated ACSS2 Peptides by LC-MS/MS. Overexpressed ACSS2-Flag was purified from SIRT2 control and knockout HEK293T cells by immunoprecipitation with anti-Flag affinity beads. The purified protein was digested with 1.5 mg of trypsin in a glass vial at 37˚C for 2 hours, and then desalted using Sep-Pak C18 cartridge. The peptides were processed as previously described[45], and data was acquired using Xcalibur 2.2 operation software.

ACSS2 activity assay. ACSS2 activity was monitored by detecting the acetyl-CoA formation using HPLC. A reaction buffer (60 mM potassium phosphate pH 7.5, 3 mM ATP, 0.1 mM CoA, 4 mM $MgCl_2$, 1 mM DTT, 0.24 mM sodium acetate) was prepared. Reactions were prepared with 0.04 μg of recombinant human ACSS2 protein. All samples were incubated at 37 °C for the indicated time after which it was quenched with 10 μl of glacial acetic acid. After vortexing and centrifuging at 17□000*g* for 5 min to remove the precipitated enzyme, the supernatant was loaded to HPLC with a Kinetex EVO C18 column (100 × 4.60 mm, 5 μM, 100 Å) for analysis. All experiments were performed in duplicate. The amount of acetyl-CoA formed over time was detected and quantified.

Data analysis. Statistical analysis was performed using Prism (Graphpad Software). Experimental values are shown as mean ±SEM. Statistical significance between two groups was determined using the two-tailed Student's t-test. One-way ANOVA was applied for multigroup comparisons. P values<0.05 were considered significant.

References

(1) Ameer, F.; Scandiuzzi, L.; Hasnain, S.; Kalbacher, H.; Zaidi, N. De Novo Lipogenesis in Health and Disease. *Metabolism* **2014**, *63* (7), 895–902. https://doi.org/10.1016/j.metabol.2014.04.003.

(2) Koundouros, N.; Poulogiannis, G. Reprogramming of Fatty Acid Metabolism in Cancer. *Br J Cancer* **2020**, *122* (1), 4–22. https://doi.org/10.1038/s41416-019-0650-z.

(3) Song, Z.; Xiaoli, A.; Yang, F. Regulation and Metabolic Significance of De Novo Lipogenesis in Adipose Tissues. *Nutrients* **2018**, *10* (10), 1383. https://doi.org/10.3390/nu10101383.

(4) Nassir, F.; Rector, R. S.; Hammoud, G. M.; Ibdah, J. A. Pathogenesis and Prevention of Hepatic Steatosis. *Gastroenterol Hepatol (N Y)* **2015**, *11* (3).

(5) Scholarlycommons, S.; Zhao, S. *From Sugar To Acetate-The Origins Of Acetyl-Coa Dictate Its Use From Sugar To Acetate-The Origins Of Acetyl-Coa Dictate Its Use In Cells And In Mice In Cells And In Mice*. https://repository.upenn.edu/edissertations.

(6) Icard, P.; Wu, Z.; Fournel, L.; Coquerel, A.; Lincet, H.; Alifano, M. ATP Citrate Lyase: A Central Metabolic Enzyme in Cancer. *Cancer Lett* **2020**, *471*, 125–134. https://doi.org/10.1016/j.canlet.2019.12.010.

(7) Feng, X.; Zhang, L.; Xu, S.; Shen, A. zong. ATP-Citrate Lyase (ACLY) in Lipid Metabolism and Atherosclerosis: An Updated Review. *Progress in Lipid Research*. 2020. https://doi.org/10.1016/j.plipres.2019.101006.

(8) Ling, R.; Chen, G.; Tang, X.; Liu, N.; Zhou, Y.; Chen, D. Acetyl-CoA Synthetase 2(ACSS2): A Review with a Focus on Metabolism and Tumor Development. *Discover Oncology* **2022**, *13* (1), 58. https://doi.org/10.1007/s12672-022-00521-1.

(9) Schug, Z. T.; Peck, B.; Jones, D. T.; Zhang, Q.; Grosskurth, S.; Alam, I. S.; Goodwin, L. M.; Smethurst, E.; Mason, S.; Blyth, K.; McGarry, L.; James, D.; Shanks, E.; Kalna, G.; Saunders, R. E.; Jiang, M.; Howell, M.; Lassailly, F.; Thin, M. Z.; Spencer-Dene, B.; Stamp, G.; van den Broek, N. J. F.; Mackay, G.; Bulusu, V.; Kamphorst, J. J.; Tardito, S.; Strachan, D.; Harris, A. L.; Aboagye, E. O.; Critchlow, S. E.; Wakelam, M. J. O.; Schulze, A.; Gottlieb, E. Acetyl-CoA Synthetase 2 Promotes Acetate Utilization and Maintains Cancer Cell Growth under Metabolic Stress. *Cancer Cell* **2015**, *27* (1), 57–71. https://doi.org/10.1016/j.ccell.2014.12.002.

(10) Schug, Z. T.; Vande Voorde, J.; Gottlieb, E. The Metabolic Fate of Acetate in Cancer. *Nature Reviews Cancer*. Nature Publishing Group October 24, 2016, pp 708–717. https://doi.org/10.1038/nrc.2016.87.

(11) Miller, K. D.; Pniewski, K.; Perry, C. E.; Papp, S. B.; Shaffer, J. D.; Velasco-Silva, J. N.; Casciano, J. C.; Aramburu, T. M.; Srikanth, Y. V. V.; Cassel, J.; Skordalakes, E.; Kossenkov, A. V.; Salvino, J. M.; Schug, Z. T. Targeting ACSS2 with a Transition-State Mimetic Inhibits Triple-Negative Breast Cancer Growth. *Cancer Res* **2021**, *81* (5). https://doi.org/10.1158/0008-5472.CAN-20-1847.

(12) Chen, R.; Xu, M.; Nagati, J. S.; Hogg, R. T.; Das, A.; Gerard, R. D.; Garcia, J. A. The Acetate/ACSS2 Switch Regulates HIF-2 Stress Signaling in the Tumor Cell Microenvironment. *PLoS One* **2015**, *10* (2). https://doi.org/10.1371/journal.pone.0116515.

(13) Gao, X.; Lin, S. H.; Ren, F.; Li, J. T.; Chen, J. J.; Yao, C. B.; Yang, H. Bin; Jiang, S. X.; Yan, G. Q.; Wang, D.; Wang, Y.; Liu, Y.; Cai, Z.; Xu, Y. Y.; Chen, J.; Yu, W.; Yang, P. Y.;

Lei, Q. Y. Acetate Functions as an Epigenetic Metabolite to Promote Lipid Synthesis under Hypoxia. *Nat Commun* **2016**, *7*. https://doi.org/10.1038/ncomms11960.

(14) Huang, Z.; Zhang, M.; Plec, A. A.; Estill, S. J.; Cai, L.; Repa, J. J.; McKnight, S. L.; Tu, B. P. ACSS2 Promotes Systemic Fat Storage and Utilization through Selective Regulation of Genes Involved in Lipid Metabolism. *Proc Natl Acad Sci U S A* **2018**, *115* (40), E9499–E9506. https://doi.org/10.1073/pnas.1806635115.

(15) Drazic, A.; Myklebust, L. M.; Ree, R.; Arnesen, T. The World of Protein Acetylation. *Biochimica et Biophysica Acta (BBA) - Proteins and Proteomics* **2016**, *1864* (10), 1372–1401. https://doi.org/10.1016/j.bbapap.2016.06.007.

(16) Park, S.-Y.; Kim, J.-S. A Short Guide to Histone Deacetylases Including Recent Progress on Class II Enzymes. *Exp Mol Med* **2020**, *52* (2), 204–212. https://doi.org/10.1038/s12276-020-0382-4.

(17) Hallows, W. C.; Lee, S.; Denu, J. M. Sirtuins Deacetylate and Activate Mammalian Acetyl-CoA Synthetases. *Proceedings of the National Academy of Sciences* **2006**, *103* (27), 10230–10235. https://doi.org/10.1073/pnas.0604392103.

(18) Sahar, S.; Masubuchi, S.; Eckel-Mahan, K.; Vollmer, S.; Galla, L.; Ceglia, N.; Masri, S.; Barth, T. K.; Grimaldi, B.; Oluyemi, O.; Astarita, G.; Hallows, W. C.; Piomelli, D.; Imhof, A.; Baldi, P.; Denu, J. M.; Sassone-Corsi, P. Circadian Control of Fatty Acid Elongation by SIRT1 Protein-Mediated Deacetylation of Acetyl-Coenzyme A Synthetase 1. *Journal of Biological Chemistry* **2014**, *289* (9), 6091–6097. https://doi.org/10.1074/jbc.M113.537191.

(19) Carafa, V.; Rotili, D.; Forgione, M.; Cuomo, F.; Serretiello, E.; Hailu, G. S.; Jarho, E.; Lahtela-Kakkonen, M.; Mai, A.; Altucci, L. Sirtuin Functions and Modulation: From Chemistry to the Clinic. *Clinical Epigenetics*. 2016. https://doi.org/10.1186/s13148-016-0224-3.

(20) Imai, S. ichiro; Guarente, L. NAD+ and Sirtuins in Aging and Disease. *Trends in Cell Biology*. Elsevier Ltd 2014, pp 464–471. https://doi.org/10.1016/j.tcb.2014.04.002.

(21) Wang, M.; Lin, H. Understanding the Function of Mammalian Sirtuins and Protein Lysine Acylation. *Annu Rev Biochem* **2021**, *90* (1), 245–285. https://doi.org/10.1146/annurev-biochem-082520-125411.

(22) Head, P. E.; Zhang, H.; Bastien, A. J.; Koyen, A. E.; Withers, A. E.; Daddacha, W. B.; Cheng, X.; Yu, D. S. Sirtuin 2 Mutations in Human Cancers Impair Its Function in Genome Maintenance. *Journal of Biological Chemistry* **2017**, *292* (24), 9919–9931. https://doi.org/10.1074/jbc.M116.772566.

(23) Wang, M.; Zhang, Y.; Komaniecki, G. P.; Lu, X.; Cao, J.; Zhang, M.; Yu, T.; Hou, D.; Spiegelman, N. A.; Yang, M.; Price, I. R.; Lin, H. Golgi Stress Induces SIRT2 to Counteract Shigella Infection via Defatty-Acylation. *Nat Commun* **2022**, *13* (1). https://doi.org/10.1038/s41467-022-32227-x.

(24) Zullo, A.; Simone, E.; Grimaldi, M.; Gagliardi, M.; Zullo, L.; Matarazzo, M. R.; Mancini, F. P. Effect of Nutrient Deprivation on the Expression and the Epigenetic Signature of Sirtuin Genes. *Nutrition, Metabolism and Cardiovascular Diseases* **2018**, *28* (4), 418–424. https://doi.org/10.1016/j.numecd.2018.02.004.

(25) Wang, F.; Tong, Q. SIRT2 Suppresses Adipocyte Differentiation by Deacetylating FOXO1 and Enhancing FOXO1's Repressive Interaction with PPAR. *Mol Biol Cell* **2009**, *20*, 801–808. https://doi.org/10.1091/mbc.E08.

(26) Ma, L.; Tao, Y.; Duran, A.; Llado, V.; Galvez, A.; Barger, J. F.; Castilla, E. A.; Chen, J.; Yajima, T.; Porollo, A.; Medvedovic, M.; Brill, L. M.; Plas, D. R.; Riedl, S. J.; Leitges, M.; Diaz-Meco, M. T.; Richardson, A. D.; Moscat, J. Control of Nutrient Stress-Induced Metabolic Reprogramming by PKCζ in Tumorigenesis. *Cell* **2013**, *152* (3), 599–611. https://doi.org/10.1016/j.cell.2012.12.028.

(27) Sun, L.; Xiong, H.; Chen, L.; Dai, X.; Yan, X.; Wu, Y.; Yang, M.; Shan, M.; Li, T.; Yao, J.; Jiang, W.; He, H.; He, F.; Lian, J. *Deacetylation of ATG4B Promotes Autophagy Initiation under Starvation*; 2022; Vol. 8.

(28) Mauvezin, C.; Neufeld, T. P. Bafilomycin A1 Disrupts Autophagic Flux by Inhibiting Both V-ATPase-Dependent Acidification and Ca-P60A/SERCA-Dependent Autophagosome-Lysosome Fusion. *Autophagy* **2015**, *11* (8), 1437–1438. https://doi.org/10.1080/15548627.2015.1066957.

(29) Zhang, L.; Tang, H.; Kou, Y.; Li, R.; Zheng, Y.; Wang, Q.; Zhou, X.; Jin, L. MG132-Mediated Inhibition of the Ubiquitin-Proteasome Pathway Ameliorates Cancer Cachexia. *J Cancer Res Clin Oncol* **2013**, *139* (7). https://doi.org/10.1007/s00432-013-1412-6.

(30) Kwon, Y. T.; Ciechanover, A. The Ubiquitin Code in the Ubiquitin-Proteasome System and Autophagy. *Trends in Biochemical Sciences*. 2017. https://doi.org/10.1016/j.tibs.2017.09.002.

(31) Kim, W.; Bennett, E. J.; Huttlin, E. L.; Guo, A.; Li, J.; Possemato, A.; Sowa, M. E.; Rad, R.; Rush, J.; Comb, M. J.; Harper, J. W.; Gygi, S. P. Systematic and Quantitative Assessment of the Ubiquitin-Modified Proteome. *Mol Cell* **2011**, *44* (2), 325–340. https://doi.org/10.1016/j.molcel.2011.08.025.

(32) Asfa, A. S.; Qiu, B.; Wee, S.; Choi, H.; Gunaratne, J.; Tergaonkar, V. Phosphoprotein Network Analysis of White Adipose Tissues Unveils Deregulated Pathways in Response to High-Fat Diet. *Sci Rep* **2016**, *6*. https://doi.org/10.1038/srep25844.

(33) Wang, Y.; Yang, J.; Hong, T.; Chen, X.; Cui, L. SIRT2: Controversy and Multiple Roles in Disease and Physiology. *Ageing Research Reviews*. Elsevier Ireland Ltd November 1, 2019. https://doi.org/10.1016/j.arr.2019.100961.

(34) Gomes, P.; Fleming Outeiro, T.; Cavadas, C. Emerging Role of Sirtuin 2 in the Regulation of Mammalian Metabolism. *Trends in Pharmacological Sciences*. 2015. https://doi.org/10.1016/j.tips.2015.08.001.

(35) Wang, F.; Tong, Q. SIRT2 Suppresses Adipocyte Differentiation by Deacetylating FOXO1 and Enhancing FOXO1's Repressive Interaction with PPAR. *Mol Biol Cell* **2009**, *20*, 801–808. https://doi.org/10.1091/mbc.E08.

(36) Hernandez-Quiles, M.; Broekema, M. F.; Kalkhoven, E. PPARgamma in Metabolism, Immunity, and Cancer: Unified and Diverse Mechanisms of Action. *Frontiers in Endocrinology*. Frontiers Media S.A. February 26, 2021. https://doi.org/10.3389/fendo.2021.624112.

(37) Lin, R.; Tao, R.; Gao, X.; Li, T.; Zhou, X.; Guan, K. L.; Xiong, Y.; Lei, Q. Y. Acetylation Stabilizes ATP-Citrate Lyase to Promote Lipid Biosynthesis and Tumor Growth. *Mol Cell* **2013**, *51* (4). https://doi.org/10.1016/j.molcel.2013.07.002.

(38) Guo, L.; Guo, Y. Y.; Li, B. Y.; Peng, W. Q.; Chang, X. X.; Gao, X.; Tang, Q. Q. Enhanced Acetylation of ATP-Citrate Lyase Promotes the Progression of Nonalcoholic Fatty Liver Disease. *Journal of Biological Chemistry* **2019**, *294* (31), 11805–11816. https://doi.org/10.1074/jbc.RA119.008708.

(39) Chen, N.; Zhao, M.; Wu, N.; Guo, Y.; Cao, B.; Zhan, B.; Li, Y.; Zhou, T.; Zhu, F.; Guo, C.; Shi, Y.; Wang, Q.; Li, Y.; Zhang, L. ACSS2 Controls PPARγ Activity Homeostasis to Potentiate Adipose-Tissue Plasticity. *Cell Death Differ* **2024**, *31* (4), 479–496. https://doi.org/10.1038/s41418-024-01262-0.

(40) Garcia, J. A.; Chen, R.; Xu, M.; Comerford, S. A.; Hammer, R. E.; Melton, S. D.; Feagins, L. A. Acss2/HIF-2 Signaling Facilitates Colon Cancer Growth and Metastasis. *PLoS One* **2023**, *18* (3), e0282223. https://doi.org/10.1371/journal.pone.0282223.

(41) Guo, F.; Cavener, D. R. The GCN2 EIF2α Kinase Regulates Fatty-Acid Homeostasis in the Liver during Deprivation of an Essential Amino Acid. *Cell Metab* **2007**, *5* (2), 103–114. https://doi.org/10.1016/j.cmet.2007.01.001.

(42) Yki-Järvinen, H.; Luukkonen, P. K.; Hodson, L.; Moore, J. B. Dietary Carbohydrates and Fats in Nonalcoholic Fatty Liver Disease. *Nature Reviews Gastroenterology and Hepatology*. Nature Research November 1, 2021, pp 770–786. https://doi.org/10.1038/s41575-021-00472-y.

(43) Jing, H.; Hu, J.; He, B.; Negrón Abril, Y. L.; Stupinski, J.; Weiser, K.; Carbonaro, M.; Chiang, Y. L.; Southard, T.; Giannakakou, P.; Weiss, R. S.; Lin, H. A SIRT2-Selective Inhibitor Promotes c-Myc Oncoprotein Degradation and Exhibits Broad Anticancer Activity. *Cancer Cell* **2016**, *29* (3), 297–310. https://doi.org/10.1016/j.ccell.2016.02.007.

(44) Jing, H.; Zhang, X.; Wisner, S. A.; Chen, X.; Spiegelman, N. A.; Linder, M. E.; Lin, H. SIRT2 and Lysine Fatty Acylation Regulate the Transforming Activity of K-Ras4a. **2017**. https://doi.org/10.7554/eLife.32436.001.

(45) Miller, S. P.; Maio, G.; Zhang, X.; Badillo Soto, F. S.; Zhu, J.; Ramirez, S. Z.; Lin, H. A Proteomic Approach Identifies Isoform-Specific and Nucleotide-Dependent RAS Interactions. *Molecular & Cellular Proteomics* **2022**, *21* (8), 100268. https://doi.org/10.1016/j.mcpro.2022.100268.